

# Dispersive Properties of High Order Nédélec/Edge Element Approximation of the Time-Harmonic Maxwell Equations

Mark Ainsworth,  
Mathematics Department,  
Strathclyde University,  
26 Richmond St.,  
Glasgow G1 1XH, Scotland  
M.Ainsworth@strath.ac.uk

April 16, 2003

## Abstract

The dispersive behaviour of high order Nédélec element approximation of the time harmonic Maxwell equations at a prescribed temporal frequency  $\omega$  on tensor product meshes of size  $h$  is analysed. A simple argument is presented showing that the discrete dispersion relation may be expressed in terms of the discrete dispersion relation for the approximation of the scalar Helmholtz equation in one dimension. An explicit form for the one dimensional dispersion relation is given, valid for arbitrary order of approximation. Explicit expressions for the leading term in the error in the regimes where (a)  $\omega h$  is small, showing that the dispersion relation is accurate to order  $2p$  for a  $p$ -th order method; and (b) in the high wave number limit where  $1 \ll \omega h$ , showing that in this case the error reduces at a super-exponential rate once the order of approximation exceeds a certain threshold which is given explicitly.

## 1 Introduction

Many physical applications of practical interest involve propagation of waves at high wave number. While there are many satisfactory schemes available for low wave number analysis, the development and analysis of good schemes for high wave number applications poses a significant challenge. The use of high order finite element and spectral element schemes for the approximation of Maxwell's equations has recently attracted much interest [13, 14]. Many of the difficulties in the use of finite element schemes can be traced to the dispersive properties, where the accumulation of phase-lag over many wavelengths leads to completely unsatisfactory results and effectively limits the range of applicability of the scheme [16]. Despite this fact, the dispersive properties of finite element schemes are relatively poorly understood. This is especially true for  $p$ -version

and spectral element schemes where the order of the scheme is increased using relatively coarse, or even fixed, meshes.

A clear understanding of the dispersive properties of a scheme is not only valuable theoretically, but may also serve as a guideline for the construction of an initial mesh and initial order of the scheme. It is desirable, particularly if adaptive refinements are to be performed, that the initial mesh and scheme provides sufficient resolution for the dispersive effects to be controlled to an extent that the approximation at least exhibits the correct qualitative behaviour of the true solution. Equally well, information on the dispersive behaviour may be used as a basis for an *a priori* assessment of the anticipated level of resources needed to resolve a problem.

The goal of the present work is to analyse the dispersive properties of high order Nédélec, or *edge*, finite element schemes for the time-harmonic Maxwell equations. Specific attention is paid to the problem of identifying the threshold on the order of the method at which the scheme begins to accurately reproduce the correct dispersive behaviour of the continuous Maxwell equations.

Several authors have considered the dispersive behaviour of finite element schemes of which the following are most pertinent to the present work. Christon [7] considered the dispersive behaviour of a variety of finite element schemes for the second-order wave equation and presented numerical comparisons between the discrete phase and group velocities and the exact values. Monk and Parrott [20] have considered the dispersive behaviour of lower order finite element methods on triangular elements for Maxwell's equations as the mesh size is reduced. Cohen and Monk [9, 10, 11] performed a dispersion analysis of Nédélec type elements for the time-dependent Maxwell equations used in conjunction with lumping of the mass matrix on tensor product meshes in two and three dimensions. One interesting conclusion was that the discrete dispersion relation could be obtained in terms of the discrete dispersion relation for approximation of the scalar Helmholtz equation in one dimension, and this was exploited to analyse the dispersive properties for methods of up to third order as the mesh size  $h$  is reduced. Here, we present a simple proof demonstrating that a similar reduction to a one dimensional analysis holds for consistent higher order Nédélec finite element schemes on tensor product meshes.

The dispersive and attenuation properties of higher order finite elements for the scalar Helmholtz equation in one dimension are considered by Thompson and Pinsky [24] for methods of up to fifth order. Numerical evidence is presented leading to the conjecture that the order  $p$  elements provide an order  $2p$  accurate approximation of the dispersion relation as the mesh size  $h \rightarrow 0$ . Here, we give an explicit, closed form for the discrete dispersion relation along with an explicit expression for the leading term in the error as  $h \rightarrow 0$ , which confirms the conjecture of Thompson and Pinsky [24].

Babuška and Ihlenburg [5, 15, 17, 18] studied the dispersive properties of higher order finite elements for the Helmholtz equation in one dimension, and obtained estimates for the accuracy in the regime where  $\omega h < 1$ . The estimates provide bounds involving generic constants. Here, we shall present an estimate for this error which is, of course, consistent with the bound derived by Babuška and Ihlenburg, but which is sharp in the sense that the leading term in the

expansion of the error is given explicitly.

## 2 Time-Harmonic Maxwell Equations

Ampère's and Faraday's equations relating the electric and magnetic fields in free space, with appropriate units, take the form

$$\frac{\partial \mathbf{E}}{\partial t} - \mathbf{curl} \mathbf{B} = \mathbf{0}; \quad \frac{\partial \mathbf{B}}{\partial t} + \mathbf{curl} \mathbf{E} = \mathbf{0}. \quad (1)$$

If, for a given temporal frequency  $\omega$ , we seek a time-harmonic solution of the form

$$\mathbf{E}(\mathbf{x}, t) = e^{i\omega t} \mathbf{E}_0(\mathbf{x}); \quad \mathbf{B}(\mathbf{x}, t) = e^{i\omega t} \mathbf{B}_0(\mathbf{x}), \quad (2)$$

then the fields  $\mathbf{E}_0$  and  $\mathbf{B}_0$  satisfy the time-harmonic Maxwell equations

$$\begin{aligned} i\omega \mathbf{E}_0 - \mathbf{curl} \mathbf{B}_0 &= \mathbf{0} \\ i\omega \mathbf{B}_0 + \mathbf{curl} \mathbf{E}_0 &= \mathbf{0}. \end{aligned} \quad (3)$$

Eliminating the magnetic field  $\mathbf{B}_0$  (or the electric field) leads to the following equation for the electric field  $\mathbf{E}_0$  (or the magnetic field):

$$-\omega^2 \mathbf{E}_0 + \mathbf{curl} \mathbf{curl} \mathbf{E}_0 = \mathbf{0}. \quad (4)$$

The dispersion relation for this equation can be derived by seeking a non-trivial plane wave solution of the form

$$\mathbf{E}_0(\mathbf{x}) = e^{i\boldsymbol{\xi} \cdot \mathbf{x}} \boldsymbol{\alpha}, \quad (5)$$

giving the condition

$$\omega^2 \boldsymbol{\alpha} + \boldsymbol{\xi} \times (\boldsymbol{\xi} \times \boldsymbol{\alpha}) = \mathbf{0}.$$

Expanding the vector products gives

$$\left( \boldsymbol{\xi} \boldsymbol{\xi}^\top + (\omega^2 - |\boldsymbol{\xi}|^2) \mathbf{I} \right) \boldsymbol{\alpha} = \mathbf{0}$$

where  $\mathbf{I}$  denotes the identity matrix, and so, for a non-trivial solution  $\boldsymbol{\alpha}$ , we require that the determinant vanishes,

$$\begin{vmatrix} \omega^2 - \xi_2^2 - \xi_3^2 & \xi_1 \xi_2 & \xi_1 \xi_3 \\ \xi_1 \xi_2 & \omega^2 - \xi_1^2 - \xi_3^2 & \xi_2 \xi_3 \\ \xi_1 \xi_3 & \xi_2 \xi_3 & \omega^2 - \xi_1^2 - \xi_2^2 \end{vmatrix} = 0,$$

which simplifies to give

$$\omega^2 (\omega^2 - \xi_1^2 - \xi_2^2 - \xi_3^2)^2 = 0. \quad (6)$$

Hence, if  $\omega$  is non-zero, we obtain the *dispersion relation*,

$$\omega^2 = |\boldsymbol{\xi}|^2. \quad (7)$$

The plane wave solutions (5) correspond to the propagation of a monochromatic wave, and have the *Bloch wave* property [22]:

$$\mathbf{E}_0(\mathbf{x} + h\mathbf{n}) = e^{ih\boldsymbol{\xi} \cdot \mathbf{n}} \mathbf{E}_0(\mathbf{x}) \quad (8)$$

for any choice of vector  $\mathbf{n}$  and scalar  $h$ .

### 3 Higher Order Nédélec (Edge) Elements

The ability of a numerical scheme to propagate discrete plane wave type solutions, discussed in the previous section, correctly has a significant impact on the quality of the approximation that will be obtained [4, 6]. One of the aims of the present work is to study this question for certain types of finite element schemes for Maxwell's equation. Before pursuing the dispersion analysis, we first describe the type of scheme we have in mind and illustrate the behaviour of the method for a model problem.

Let  $\Omega \subset \mathbb{R}^d$ ,  $d = 2$  or  $3$  be a polyhedral domain. The appropriate function space setting for the Maxwell equations is denoted by  $\mathbf{H}(\mathbf{curl}; \Omega)$  and is defined by

$$\mathbf{H}(\mathbf{curl}; \Omega) = \left\{ \mathbf{v} \in L_2(\Omega)^d : \mathbf{curl} \mathbf{v} \in L_2(\Omega) \right\}. \quad (9)$$

One of the main features of this space that impacts the choice of a finite element discretisation is that it is only necessary for the tangential components of a field  $\mathbf{v}$  to be continuous across element interfaces. That is to say, there is no obligation for the normal components to be continuous. In fact, it is known that if standard conforming finite elements are used to discretise the problem, then it is possible for the sequence of approximations to converge to an incorrect solution of the problem unless a regularised variational formulation is employed [12]. Consequently, finite elements have been derived that respect the minimal conformity conditions imposed by the underlying space  $\mathbf{H}(\mathbf{curl}; \Omega)$ . One particular variant is due to Nédélec [21] and is often dubbed as 'edge' elements in the engineering literature.

Let  $\mathcal{M}$  be a partitioning of  $\Omega$  into curvilinear quadrilaterals or hexahedra [8], such that the non-empty intersection of distinct elements is either a single common face, edge or vertex of both elements. Each element  $K \in \mathcal{M}$  is the image of a reference element  $\widehat{K} = (-1, 1)^d$  under a differentiable bijection  $\mathbf{F}_K : \widehat{K} \rightarrow K$ . A finite element in the sense of Ciarlet [8] is represented by a triple  $(\mathcal{P}, K, \Sigma)$ . The space  $\widehat{\mathcal{P}}$  associated with the Nédélec element of order  $p$  on the reference element is given by

$$\widehat{\mathcal{P}} = \begin{cases} \mathbb{Q}_{p,p+1} \times \mathbb{Q}_{p+1,p}, & d = 2 \\ \mathbb{Q}_{p,p+1,p+1} \times \mathbb{Q}_{p+1,p,p+1} \times \mathbb{Q}_{p+1,p+1,p} & d = 3 \end{cases}$$

where

$$\mathbb{Q}_{p,q} = \{x^i y^j : 0 \leq i \leq p, 0 \leq j \leq q\}$$

and

$$\mathbb{Q}_{p,q,r} = \{x^i y^j z^k : 0 \leq i \leq p, 0 \leq j \leq q, 0 \leq k \leq r\}.$$

The set of degrees of freedom  $\widehat{\Sigma}$  is specified implicitly by the choice of basis. Let  $\{L_i\}_{i=0}^p$  denote normalised Legendre polynomials, so that  $\|L_i\|_{(-1,1)} = 1$ , and define the set  $\{\ell_i\}_{i=0}^{p+1}$  as follows

$$\ell_0(s) = \frac{1}{2}(1-s); \quad \ell_1(s) = \frac{1}{2}(1+s)$$

and

$$\ell_i(s) = \int_{-1}^s L_{i-1}(t) dt, \quad i = 2, \dots, p+1.$$

The basis functions on the quadrilateral reference element  $\widehat{K} = (-1, 1)^2$  are chosen to be

$$\left. \begin{array}{l} L_i(\xi_1)\ell_j(\xi_2)\mathbf{e}_1 \\ \ell_j(\xi_1)L_i(\xi_2)\mathbf{e}_2 \end{array} \right\} \quad i = 0, \dots, p; j = 0, \dots, p+1 \quad (10)$$

whilst for the hexahedral reference element  $\widehat{K} = (-1, 1)^3$ , the basis functions are given by

$$\left. \begin{array}{l} L_i(\xi_1)\ell_j(\xi_2)\ell_k(\xi_3)\mathbf{e}_1 \\ \ell_j(\xi_1)L_i(\xi_2)\ell_k(\xi_3)\mathbf{e}_2 \\ \ell_j(\xi_1)\ell_k(\xi_2)L_i(\xi_3)\mathbf{e}_3 \end{array} \right\} \quad i = 0, \dots, p; j, k = 0, \dots, p+1 \quad (11)$$

where  $\mathbf{e}_1, \dots, \mathbf{e}_3$  denote the unit Cartesian vectors. The dimensions of  $\widehat{\mathcal{P}}$  are given by  $d(p+1)(p+2)^{d-1}$  for  $d = 2, 3$ .

The Nédélec element  $(\mathcal{P}, K, \Sigma)$  on a physical domain  $K$  is constructed from the reference element as follows. First, observe that the electric field  $\widehat{\mathbf{E}}$  on a reference element is related to the field  $\mathbf{E}$  on the physical element by the *covariant* transformation [19],

$$\mathbf{E}(\mathbf{x})|_K = \mathbf{J}_K^{-\top} \widehat{\mathbf{E}}(\boldsymbol{\xi}), \quad \mathbf{x} = \mathbf{F}_K(\boldsymbol{\xi}). \quad (12)$$

Consequently, the global basis function  $\phi$  corresponding to the local basis function  $\widehat{\phi}$  on the reference element is defined by

$$\phi(\mathbf{x})|_K = \mathbf{J}_K^{-\top} \widehat{\phi}(\boldsymbol{\xi}). \quad (13)$$

The degrees of freedom  $\Sigma$  on the global element are implicit in the choice of basis. The degrees of freedom shared by more than one element may be shown to correspond to tangential moments of the field on the edges and faces of the element [21].

One feature of the basis presented above that is important for efficient practical implementation is that it is *hierarchical*. An alternative hierarchical basis will be found in [23]. However, numerical evidence presented in [2] indicates that the latter choice leads to extremely poorly conditioned matrices. In fact, numerical evidence suggests that the condition number degenerates exponentially fast with the polynomial order  $p$ . The conditioning of the basis described above is analysed in [3].

In order to illustrate the performance of higher order elements, we consider the simple problem of the numerical propagation of a plane wave across a square domain  $\Omega = (0, 1)^2$ . Let  $\omega$  be fixed, then for given sufficiently smooth data  $g$ , we wish to approximate:  $\mathbf{E} \in \mathbf{H}(\mathbf{curl}; \Omega)$  such that

$$(\mathbf{curl} \mathbf{E}, \mathbf{curl} \mathbf{v}) - \omega^2 (\mathbf{E}, \mathbf{v}) = 0 \quad (14)$$

for all  $\mathbf{v} \in \mathbf{H}_0(\mathbf{curl}; \Omega)$ , subject to the essential boundary conditions

$$\mathbf{t} \cdot \mathbf{E} = g \text{ on } \partial\Omega, \quad (15)$$

where  $\mathbf{t}$  is the unit tangent on the boundary  $\partial\Omega$ . Here, we adopt the usual convention in two dimensions and denote

$$\mathbf{curl} \psi = \left( \frac{\partial \psi}{\partial y}, \frac{\partial \psi}{\partial x} \right); \quad \mathbf{curl} \mathbf{v} = \frac{\partial v_2}{\partial x} - \frac{\partial v_1}{\partial y}.$$

Let  $\tilde{\mathbf{E}} = i \mathbf{curl}(\exp(i\mathbf{k} \cdot \mathbf{x}))$  denote the plane wave propagating in the direction  $\mathbf{k} = 4\pi(1, 1)$ . If the data are chosen so that  $g = \mathbf{t} \cdot \tilde{\mathbf{E}}$  and  $\omega^2 = 8\pi^2$ , then  $\tilde{\mathbf{E}}$  is the exact solution of the problem.

The domain is subdivided into a uniform mesh of square elements of size  $h$ , and Nédélec elements of uniform order  $p$  are used to define the finite element space  $\mathbf{V}_{hp}$ . The finite element approximation  $\mathbf{E}_{hp} \in \mathbf{V}_{hp}$  is sought such that

$$(\mathbf{curl} \mathbf{E}_{hp}, \mathbf{curl} \mathbf{v}) - \omega^2 (\mathbf{E}_{hp}, \mathbf{v}) = 0 \quad (16)$$

for all  $\mathbf{v} \in \mathbf{V}_{hp} \cap \mathbf{H}_0(\mathbf{curl}; \Omega)$ . The essential boundary conditions are applied by requiring that on every element edge  $\gamma \subset \partial\Omega$ :

$$\int_{\gamma} (\mathbf{t} \cdot \mathbf{E}_{hp} - g) v \, ds = 0 \quad (17)$$

for all  $v \in \mathbb{P}_p(\gamma)$ , where  $\mathbb{P}_p$  denotes polynomials of degree at most  $p$  in the arc-length.

The problem is approximated using two alternative approaches: either the  $h$ -version finite element method where uniform mesh refinement is performed in conjunction with the low order Nédélec elements, or, the  $p$ -version finite element method where a single element is used in conjunction with uniform increase in the order  $p$  of the elements.

Fig. 1 shows the second component of the approximation to the electric field obtained using first order Nédélec elements. Recall that for an  $\mathbf{H}(\mathbf{curl})$ -conforming approximation only the continuity of the tangential component of the electric field is enforced, whilst the normal component of the field may be discontinuous, as shown in Fig. 1.

In order to study the dispersive behaviour of each type of scheme, the variation of the component of the true and approximate solutions in the direction  $(1, 1)$  along the leading diagonal is shown for both  $h$ -version and  $p$ -version approximation.

Fig. 2 shows the results obtained using lowest order Nédélec elements and  $h$ -refinement on a sequence of uniform meshes. A mesh of  $32 \times 32$  elements (i.e. 2112 degrees of freedom) is needed to provide an accurate resolution of the wave.

Fig. 3 shows the results obtained by increasing the order of the scheme to first order Nédélec elements and  $h$ -refinement on a sequence of uniform meshes. Here, a coarser mesh of  $16 \times 16$  elements, again requiring 2112 degrees of freedom, provides good resolution of the wave.

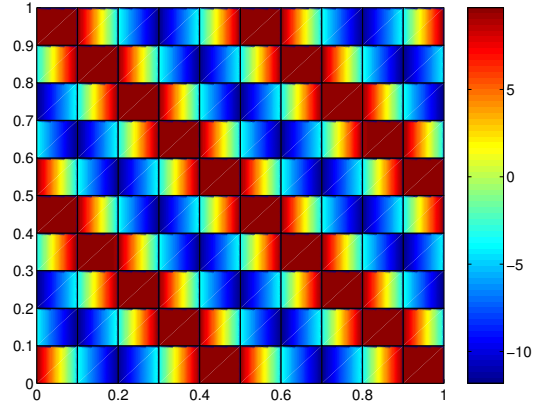


Figure 1: Second component,  $E_y$ , of electric field obtained using a 10x10 grid and first order Nédélec elements.

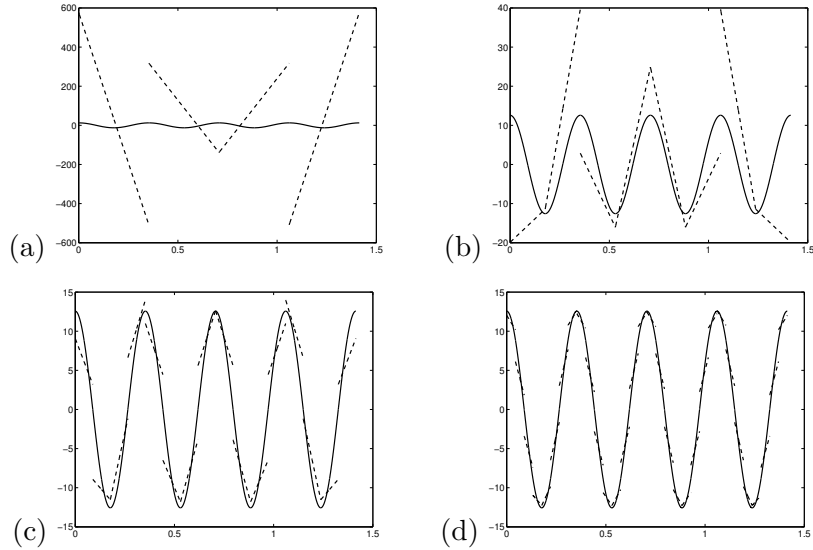


Figure 2: Variation of (1,1) component of true (solid line) and approximate (dashed line) solutions along leading diagonal for  $h$ -version approximation using zeroth order Nédélec elements. (a)  $h = 1/4$ . (b)  $h = 1/8$ . (c)  $h = 1/16$ . (d)  $h = 1/32$ .

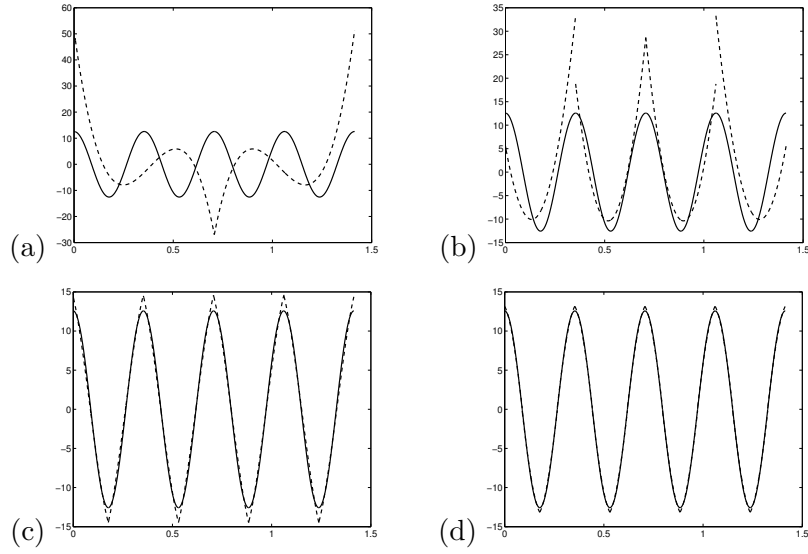


Figure 3: Variation of (1,1) component of true (solid line) and approximate (dashed line) solutions along leading diagonal for  $h$ -version approximation using first order Nédélec elements. (a)  $h = 1/2$ . (b)  $h = 1/4$ . (c)  $h = 1/8$ . (d)  $h = 1/16$ .

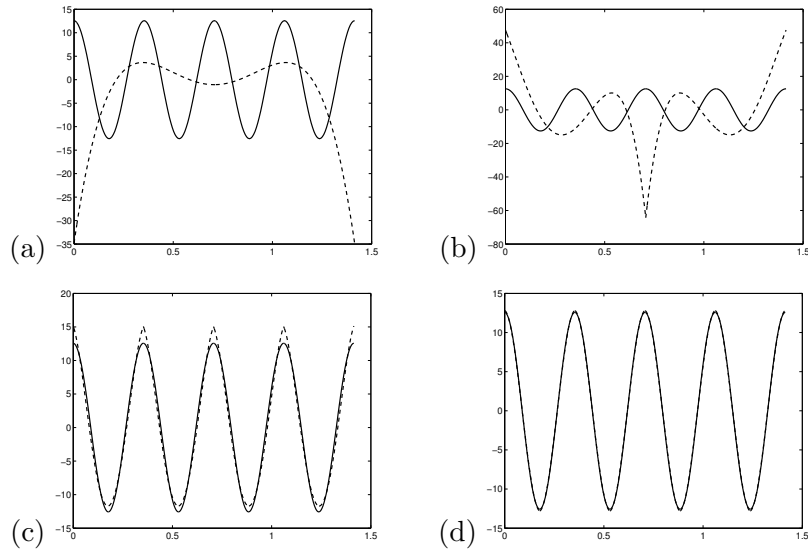


Figure 4: Variation of (1,1) component of true (solid line) and approximate (dashed line) solutions along leading diagonal for  $h$ -version approximation using second order Nédélec elements. (a)  $h = 1$ . (b)  $h = 1/2$ . (c)  $h = 1/4$ . (d)  $h = 1/8$ .



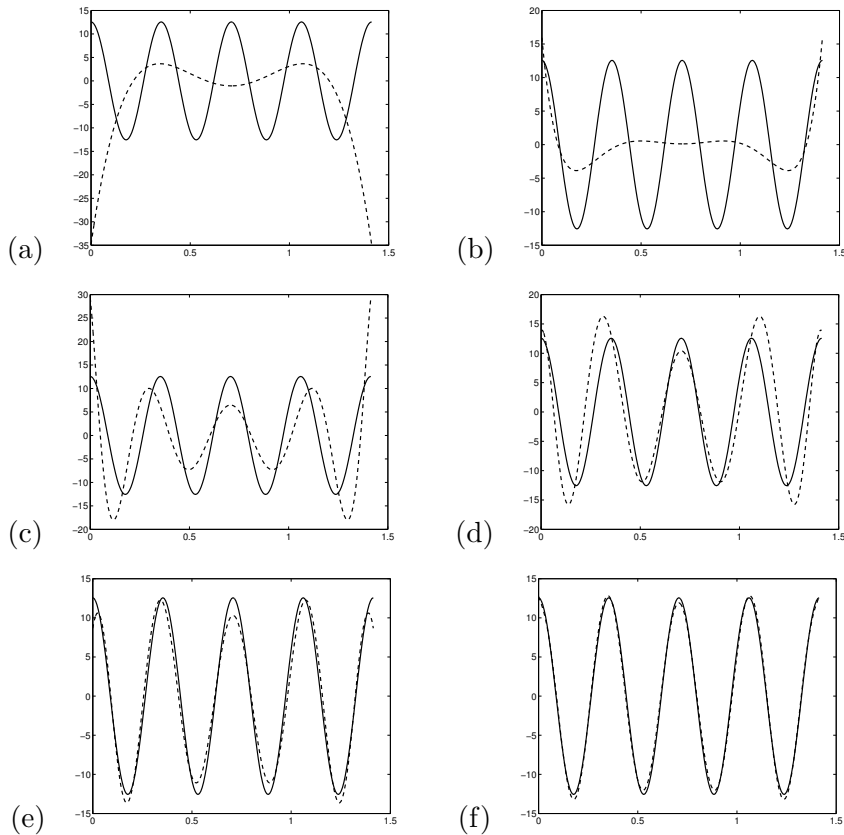


Figure 5: Variation of  $(1, 1)$  component of true and approximate solutions along leading diagonal for  $p$ -version approximation on a single element. (a)  $p = 2$ . (b)  $p = 4$ . (c)  $p = 5$ . (d)  $p = 6$ . (e)  $p = 7$ . (f)  $p = 8$ .

Fig. 4 shows the results obtained by further increasing the order of the scheme to second order Nédélec elements. Once again, a coarser mesh of  $8 \times 8$  elements (i.e. 1200 degrees of freedom) gives good resolution of the wave.

These results suggest an alternative strategy whereby the mesh is fixed, and the order  $p$  of the scheme is increased. Fig. 5 shows the results obtained using the  $p$ -version on a single element. The initial second order approximation provides poor resolution, but this rapidly improves as the order is increased. The number of degrees of freedom needed for  $p$ -th order approximation on a single element is given by  $2(p+1)(p+2)$ , meaning that only 180 degrees of freedom are needed for  $p = 8$ .

For comparison, the results of using a  $p$ -version on a  $2 \times 2$  mesh are shown Fig. 6. Once again, the initial zeroth order approximation provides poor resolution, but this rapidly improves as the order is increased.

The numerical example considered above compares the effect of mesh refinement versus  $p$ -refinement for the resolution of a simple plane wave. It is found that the  $p$ -version gives very rapid convergence once the order is sufficiently high to resolve the wave, and involves significantly fewer degrees of freedom. In

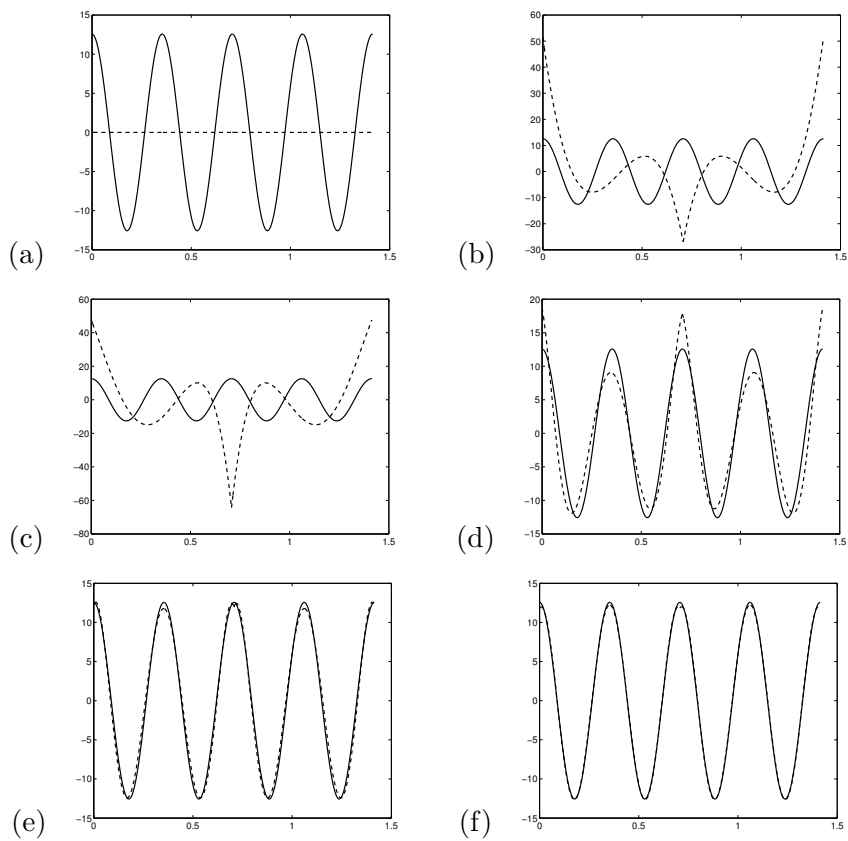


Figure 6: Variation of  $(1, 1)$  component of true and approximate solutions along leading diagonal for  $p$ -version approximation on a  $2 \times 2$  mesh. (a)  $p = 0$ . (b)  $p = 1$ . (c)  $p = 2$ . (d)  $p = 3$ . (e)  $p = 4$ . (f)  $p = 5$ .

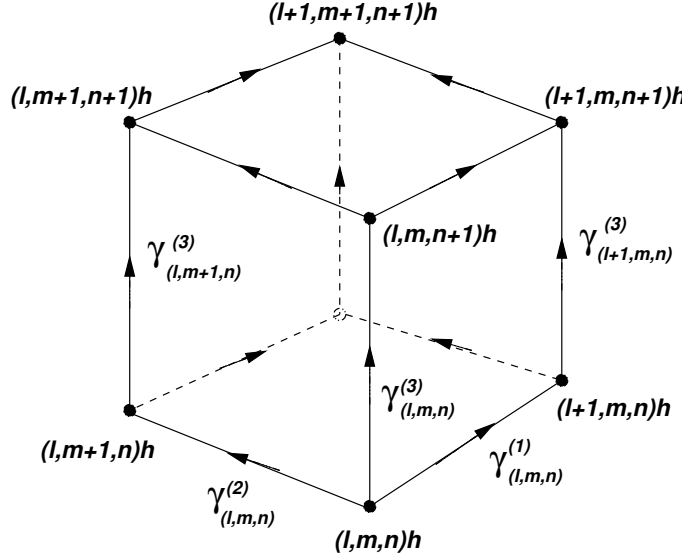


Figure 7: Notation used to describe edges relative to vertices for a typical element drawn from an infinite mesh of uniform, cubic elements of size  $h$ . The orientation associated with the degrees of freedom for the lowest order Nédélec elements is indicated by arrows.

subsequent sections, we shall investigate this behaviour analytically.

## 4 Discrete Dispersion for Lowest Order Nédélec Elements

For ease of exposition, we begin by discussing the dispersive properties of lowest order Nédélec elements. Suppose that free space is partitioned into an infinite, uniform mesh consisting of cubes of size  $h$ , with Cartesian coordinate axes chosen to coincide with the directions of edges of the cubes. A typical element is shown in Fig. 7. Let  $\mathbf{V}_h$  denote the lowest order Nédélec elements constructed on this mesh. Any function  $\mathbf{E}_h \in \mathbf{V}_h$  may be assumed, without loss of generality, to have  $d$ -th spatial component of the form

$$E_h^{(d)} = \sum_{\mathbf{n} \in \mathbb{Z}^3} \alpha_{\mathbf{n}}^{(d)} \phi_{\mathbf{n}}^{(d)} \quad (18)$$

where

$$\phi_{\mathbf{n}}^{(1)} = \begin{bmatrix} \chi_{n1}(x_1) \theta_{n2}(x_2) \theta_{n3}(x_3) \\ 0 \\ 0 \end{bmatrix} \quad (19)$$

with analogous expressions for the remaining components. Here,  $\chi_n$  is the (discontinuous) characteristic function for the interval  $(n, n+1)h$  given by

$$\chi_n(s) = \begin{cases} 1, & \text{if } s \in (nh, nh+h) \\ 0, & \text{otherwise} \end{cases} \quad (20)$$

while  $\theta_n$  is the familiar continuous, piecewise linear hat function given by

$$\theta_n(s) = \begin{cases} 1 - (n - s/h), & s \in (nh - h, nh] \\ 1 + (n - s/h), & s \in (nh, nh + 1) \\ 0, & \text{otherwise.} \end{cases} \quad (21)$$

The line integral of a typical basis function,  $\phi_{\mathbf{n}}^{(d)} \in \mathbf{V}_h$ , taken along element edges has the following simple form:

$$\int_{\gamma_{\mathbf{m}}^{(e)}} \phi_{\mathbf{n}}^{(d)} \cdot d\mathbf{x} = \begin{cases} h & \text{if } \mathbf{m} = \mathbf{n} \text{ and } d = e \\ 0 & \text{otherwise} \end{cases} \quad (22)$$

where  $\gamma_{\mathbf{m}}^{(d)}$  denotes the edge aligned with the  $d$ -th coordinate axis starting at the node indexed by  $\mathbf{m}$  (see Fig. 7). Exploiting this property allows the coefficients  $\alpha_{\mathbf{n}}^{(d)}$  to be written explicitly in terms of the field  $\mathbf{E}_h$  as follows:

$$\alpha_{\mathbf{n}}^{(d)} = \frac{1}{h} \int_{\gamma_{\mathbf{n}}^{(d)}} \mathbf{E}_h \cdot d\mathbf{x}. \quad (23)$$

By analogy with (8), a non-trivial discrete solution  $\mathbf{E}_h$  is sought which satisfies the condition

$$\mathbf{E}_h(\mathbf{x} + h\mathbf{n}) = e^{ih\boldsymbol{\xi}_h \cdot \mathbf{n}} \mathbf{E}_h(\mathbf{x}) \quad \forall \mathbf{n} \in \mathbb{Z}^3 \quad (24)$$

where  $\boldsymbol{\xi}_h$  is the discrete wave vector related to a prescribed temporal frequency  $\omega$  by the *discrete dispersion relation*. Our goal in this section is to determine the discrete dispersion relation explicitly.

Applying a change of variable in equation (23) and exploiting the translation invariance of the mesh, we deduce that

$$\begin{aligned} \alpha_{\mathbf{n}}^{(d)} &= \frac{1}{h} \int_{\gamma_{\mathbf{n}}^{(d)}} \mathbf{E}_h(\mathbf{x}) \cdot d\mathbf{x} \\ &= \frac{1}{h} \int_{\gamma_{\mathbf{0}}^{(d)}} \mathbf{E}_h(\mathbf{x} + \mathbf{n}h) \cdot d\mathbf{x} \\ &= \frac{1}{h} \int_{\gamma_{\mathbf{0}}^{(d)}} e^{ih\boldsymbol{\xi}_h \cdot \mathbf{n}} \mathbf{E}_h(\mathbf{x}) \cdot d\mathbf{x} \end{aligned}$$

and hence

$$\alpha_{\mathbf{n}}^{(d)} = e^{ih\boldsymbol{\xi}_h \cdot \mathbf{n}} \alpha_{\mathbf{0}}^{(d)} \quad \forall \mathbf{n} \in \mathbb{Z}. \quad (25)$$

Inserting condition (25) into the expression (18) gives

$$\mathbf{E}_h^{(d)} = \alpha_{\mathbf{0}}^{(d)} \sum_{\mathbf{n} \in \mathbb{Z}^3} e^{ih\boldsymbol{\xi}_h \cdot \mathbf{n}} \phi_{\mathbf{n}}^{(d)}, \quad (26)$$

and then, exploiting the fact that the summand decouples into separate contributions from each component of  $\mathbf{n}$ , it follows that

$$\begin{aligned} E_h^{(1)} &= \alpha_{\mathbf{0}}^{(1)} \Upsilon_h(\xi_1; x_1) \Theta_h(\xi_2; x_2) \Theta_h(\xi_3; x_3) \\ E_h^{(2)} &= \alpha_{\mathbf{0}}^{(2)} \Theta_h(\xi_1; x_1) \Upsilon_h(\xi_2; x_2) \Theta_h(\xi_3; x_3) \\ E_h^{(3)} &= \alpha_{\mathbf{0}}^{(3)} \Theta_h(\xi_1; x_1) \Theta_h(\xi_2; x_2) \Upsilon_h(\xi_3; x_3) \end{aligned} \quad (27)$$

where

$$\Upsilon_h(\xi; s) = \sum_{n \in \mathbb{Z}} e^{ih\xi n} \chi_n(s) \quad (28)$$

and

$$\Theta_h(\xi; s) = \sum_{n \in \mathbb{Z}} e^{ih\xi n} \theta_n(s). \quad (29)$$

Equation (27) is the discrete analogue of equation (5) and reflects the fact that both the discrete and continuous fields have only three degrees of freedom, corresponding to the scalings applied to the individual components of the discrete solution.

The functions  $\Theta_h$  and  $\Upsilon_h$  have several interesting properties. Let  $V_h$  denote the space of continuous, piecewise linear functions on the real line with nodes located at  $h\mathbb{Z}$ . The function  $\Theta_h(\xi; \cdot)$  may be regarded as the discrete analogue of the complex exponential  $e^{i\xi s}$ . For instance,  $\Theta_h(\xi; \cdot) \in V_h$  is the interpolant to the complex exponential at the nodes and satisfies

$$\Theta_h(\xi; s + nh) = e^{ih\xi n} \Theta_h(\xi; s) \quad \forall n \in \mathbb{Z}. \quad (30)$$

Moreover,  $\Theta_h(\xi; \cdot)$  satisfies the discrete variational counterpart of the eigenvalue problem satisfied by the complex exponential function  $-(e^{i\xi s})'' = \xi^2 e^{i\xi s}$ , namely,

$$\int_{\mathbb{R}} \Theta_h(\xi; s)' v_h'(s) ds = \omega_h(\xi)^2 \int_{\mathbb{R}} \Theta_h(\xi; s) v_h(s) ds \quad \forall v_h \in V_h \quad (31)$$

where a simple computation shows that the eigenvalue is given by

$$\omega_h(\xi)^2 = \frac{6}{h^2} \frac{1 - \cos(h\xi)}{2 + \cos(h\xi)} = \xi^2 \left( 1 + \frac{1}{12}(h\xi)^2 + \dots \right). \quad (32)$$

This result is well-known, e.g. Thompson and Pinsky [24], and represents the *discrete dispersion relation* for the scalar Helmholtz equation in one dimension  $u'' + \omega^2 u = 0$ :

$$\omega^2 = \xi^2.$$

The function  $\Upsilon_h(\xi; \cdot)$  is also closely related to the complex exponential  $e^{i\xi s}$ . For instance, the complex exponential satisfies  $(e^{i\xi s})' = i\xi e^{i\xi s}$ . An elementary computation reveals the following discrete counterpart of this property:

$$\Theta_h'(\xi; \cdot) = \Delta(\xi; h) \Upsilon_h(\xi; \cdot) \quad (33)$$

where

$$\Delta(\xi; h) = \frac{e^{ih\xi} - 1}{h} \rightarrow i\xi \text{ as } h\xi \rightarrow 0. \quad (34)$$

This property means that the function  $\mathbf{E}_h$  defined by equation (27) may be expressed in the alternative form

$$\begin{aligned} E_h^{(1)} &= \alpha_1 \Theta_h'(\xi_1; x_1) \Theta_h(\xi_2; x_2) \Theta_h(\xi_3; x_3) \\ E_h^{(2)} &= \alpha_2 \Theta_h(\xi_1; x_1) \Theta_h'(\xi_2; x_2) \Theta_h(\xi_3; x_3) \\ E_h^{(3)} &= \alpha_3 \Theta_h(\xi_1; x_1) \Theta_h(\xi_2; x_2) \Theta_h'(\xi_3; x_3) \end{aligned} \quad (35)$$

where  $\alpha_1 = \alpha_{\mathbf{0}}^{(1)}/\Delta(\xi_1; h)$  etc.

In order to determine the discrete dispersion relation, a non-trivial discrete solution of the form (35) is sought which satisfies the variational form of (4):

$$(\mathbf{curl} \mathbf{E}_h, \mathbf{curl} \mathbf{v}_h) - \omega^2(\mathbf{E}_h, \mathbf{v}_h) = 0 \text{ for all } \mathbf{v}_h \in \mathbf{V}_h. \quad (36)$$

At first sight, this problem seems to be intractable since there are only three degrees of freedom associated with the function  $\mathbf{E}_h$  given by (35), while equation (36) appears to embody infinitely many conditions. However, the translation invariance of the mesh means that equation (4) really only imposes three independent conditions, as shown by the following arguments.

Firstly, for any  $\mathbf{n} \in \mathbb{Z}^3$ , choose  $\mathbf{v}_h \in \mathbf{V}_h$  of the form

$$\mathbf{v}_h = \begin{bmatrix} \theta'_{n1}(x_1) \theta_{n2}(x_2) \theta_{n3}(x_3) \\ 0 \\ 0 \end{bmatrix} \quad (37)$$

then an elementary computation using property (31) reveals that

$$(\mathbf{E}_h, \mathbf{v}_h) = \omega_h(\xi_1)^2 \alpha_1 \prod_{\ell=1}^3 \int_{\mathbb{R}} \Theta_h(\xi_\ell; s) \theta_{n\ell}(s) ds \quad (38)$$

and

$$\begin{aligned} (\mathbf{curl} \mathbf{E}_h, \mathbf{curl} \mathbf{v}_h) &= \prod_{\ell=1}^3 \int_{\mathbb{R}} \Theta_h(\xi_\ell; s) \theta_{n\ell}(s) ds \times \\ &\omega_h(\xi_1)^2 [\alpha_1(\omega_h(\xi_2)^2 + \omega_h(\xi_3)^2) - \alpha_2\omega_h(\xi_2)^2 - \alpha_3\omega_h(\xi_3)^2]. \end{aligned} \quad (39)$$

Hence, with this choice of  $\mathbf{v}_h$ , equation (36) simplifies to the algebraic condition

$$\omega(\xi_1)^2 [\alpha_1(\omega_h(\xi_2)^2 + \omega_h(\xi_3)^2 - \omega^2) - \alpha_2\omega_h(\xi_2)^2 - \alpha_3\omega_h(\xi_3)^2] = 0. \quad (40)$$

Observe that the *same* algebraic condition arises regardless of the choice of multi-index  $\mathbf{n} \in \mathbb{Z}^3$ . The same argument applies to the remaining two components. Therefore, as stated above, equation (36) reduces to only three independent conditions. Consequently, we arrive at the following equivalent condition for the existence of a non-trivial solution  $\mathbf{E}_h$ :

$$\begin{vmatrix} \omega^2 - \omega_h(\xi_2)^2 - \omega_h(\xi_3)^2 & \omega_h(\xi_1)\omega_h(\xi_2) & \omega_h(\xi_1)\omega_h(\xi_3) \\ \omega_h(\xi_1)\omega_h(\xi_2) & \omega^2 - \omega_h(\xi_1)^2 - \omega_h(\xi_3)^2 & \omega_h(\xi_2)\omega_h(\xi_3) \\ \omega_h(\xi_1)\omega_h(\xi_3) & \omega_h(\xi_2)\omega_h(\xi_3) & \omega^2 - \omega_h(\xi_1)^2 - \omega_h(\xi_2)^2 \end{vmatrix} = 0.$$

Expanding and simplifying the determinant gives

$$\omega^2 (\omega^2 - \omega_h(\xi_1)^2 - \omega_h(\xi_2)^2 - \omega_h(\xi_3)^2)^2 = 0$$

and hence, for non-zero  $\omega$ , we obtain

$$\omega^2 = \omega_h(\xi_1)^2 + \omega_h(\xi_2)^2 + \omega_h(\xi_3)^2. \quad (41)$$

Inserting expression (32) leads to an explicit expression for the *discrete dispersion relation* corresponding to the lowest order Nédélec elements:

$$\omega^2 = \frac{6}{h^2} \left[ \frac{1 - \cos(h\xi_1)}{2 + \cos(h\xi_1)} + \frac{1 - \cos(h\xi_2)}{2 + \cos(h\xi_2)} + \frac{1 - \cos(h\xi_3)}{2 + \cos(h\xi_3)} \right]. \quad (42)$$

If  $h|\boldsymbol{\xi}_h| \ll 1$ , then we obtain

$$\omega^2 = |\boldsymbol{\xi}_h|^2 + \frac{h^2}{12} (\xi_1^4 + \xi_2^4 + \xi_3^4) + \dots \quad (43)$$

which exhibits the second order accuracy of the discrete dispersion relation for the lowest order Nédélec space.

The foregoing arguments show that the dispersion relation for Maxwell's equations for certain finite element schemes in higher dimensions is related to the dispersion relation in one dimension. An alternative derivation of the corresponding result for the lowest order Nédélec elements in two dimensions from first principles was given in [2].

## 5 Dispersion Relation for Nédélec Elements of Arbitrary Order

The purpose of this section is to derive the discrete dispersion relation for the space  $\mathbf{V}_{hp}$  of Nédélec elements of arbitrary order  $p \in \mathbb{N}$ , again on a partitioning of  $\mathbb{R}^3$  into uniform cubes of size  $h$ .

The key to the derivation of the dispersion relation for first order elements was the construction of the function  $\Theta_h(\xi; \cdot)$  satisfying conditions (30) and (31). Let  $V_{hp}$  denote the space of continuous, piecewise polynomials of degree  $p$  on the real line with nodes located at  $h\mathbb{Z}$ . By analogy with the lowest order case, we seek a piecewise polynomial  $\Theta_{hp}(\xi; \cdot) \in V_{hp}$  satisfying the following generalisations of properties (30) and (31):

$$\Theta_{hp}(\xi; s + nh) = e^{ih\xi n} \Theta_{hp}(\xi; s) \quad \forall n \in \mathbb{Z} \quad (44)$$

and

$$\int_{\mathbb{R}} \Theta'_{hp}(\xi; s) v'_{hp}(s) ds = \omega_{hp}(\xi)^2 \int_{\mathbb{R}} \Theta_{hp}(\xi; s) v_{hp}(s) ds \quad \forall v_{hp} \in V_{hp}. \quad (45)$$

The existence of such a function is analysed in [1] along with the dependence of  $\omega_{hp}(\xi)$  on  $\xi$ , and will be discussed in detail later.

By analogy with equation (35), for given  $\boldsymbol{\xi}_{hp} \in \mathbb{R}^3$ , define  $\mathbf{E}_{hp} \in \mathbf{V}_{hp}$  by

$$\begin{aligned} E_{hp}^{(1)} &= \alpha_1 \Theta'_{hp}(\xi_1; x_1) \Theta_{hp}(\xi_2; x_2) \Theta_{hp}(\xi_3; x_3) \\ E_{hp}^{(2)} &= \alpha_2 \Theta_{hp}(\xi_1; x_1) \Theta'_{hp}(\xi_2; x_2) \Theta_{hp}(\xi_3; x_3) \\ E_{hp}^{(3)} &= \alpha_3 \Theta_{hp}(\xi_1; x_1) \Theta_{hp}(\xi_2; x_2) \Theta'_{hp}(\xi_3; x_3), \end{aligned} \quad (46)$$

observe that, by property (44),  $\mathbf{E}_{hp}$  satisfies

$$\mathbf{E}_{hp}(\mathbf{x} + h\mathbf{n}) = e^{ih\xi_{hp}\cdot\mathbf{n}}\mathbf{E}_{hp}(\mathbf{x}) \quad \forall \mathbf{n} \in \mathbb{Z}^3. \quad (47)$$

Let  $v_1, v_2, v_3 \in V_{hp}$  be arbitrary and define  $\mathbf{v}_{hp} \in \mathbf{V}_{hp}$  by

$$\mathbf{v}_{hp} = \begin{bmatrix} v_1'(x_1) & v_2(x_2) & v_3(x_3) \\ & 0 & \\ & & 0 \end{bmatrix}, \quad (48)$$

then, similarly to the case of first order elements, property (45) again implies that

$$(\mathbf{E}_h, \mathbf{v}_h) = \omega_{hp}(\xi_1)^2 \alpha_1 \prod_{\ell=1}^3 \int_{\mathbb{R}} \Theta_{hp}(\xi_\ell; s) v_\ell(s) ds \quad (49)$$

and

$$\begin{aligned} (\mathbf{curl} \mathbf{E}_h, \mathbf{curl} \mathbf{v}_h) &= \prod_{\ell=1}^3 \int_{\mathbb{R}} \Theta_{hp}(\xi_\ell; s) v_\ell(s) ds \quad \times \\ &\omega_{hp}(\xi_1)^2 [\alpha_1(\omega_{hp}(\xi_2)^2 + \omega_{hp}(\xi_3)^2) - \alpha_2\omega_{hp}(\xi_2)^2 - \alpha_3\omega_{hp}(\xi_3)^2]. \end{aligned} \quad (50)$$

The remaining steps in the argument are identical to those used for first order elements, leading to the *discrete dispersion relation* for higher order elements

$$\omega^2 = \omega_{hp}(\xi_1)^2 + \omega_{hp}(\xi_2)^2 + \omega_{hp}(\xi_3)^2. \quad (51)$$

Cohen and Monk [9] used a quite different argument showing that a similar result holds for Gauss-point mass-lumped schemes for arbitrary order of approximation. The approach described above is more natural and is readily extended to include mass-lumped schemes.

In order to make use of equation (51), we would like to be able to express  $\omega_{hp}(\xi)$  in terms of  $\xi$ . As a matter of fact, it turns out to be easier to find an implicit definition for  $\omega_{hp}(\xi)$  in terms of  $\cos(h\xi)$ . For example, in the case of lowest order elements, the relation (32) may be rewritten in the form

$$\cos(h\xi) = R_1(h\omega_h) = \frac{6 - 2(h\omega_h)^2}{6 + (h\omega_h)^2}. \quad (52)$$

This expression is generalised to arbitrary order  $p$  in [1]:

**Theorem 1** *Let  $[2N_e + 2/2N_e]_{\kappa \tan \kappa}$  and  $[2N_o/2N_o - 2]_{\kappa \cot \kappa}$  denote the Padé approximants to  $\kappa \tan \kappa$  and  $\kappa \cot \kappa$  respectively, where  $N_e = \lfloor p/2 \rfloor$  and  $N_o = \lfloor (p+1)/2 \rfloor$ . Then,  $\omega_{hp}$  satisfies*

$$\cos(h\xi) = R_p(h\omega_{hp}) \quad (53)$$

where  $R_p$  is the rational function

$$R_p(2\kappa) = \frac{[2N_o/2N_o - 2]_{\kappa \cot \kappa} - [2N_e + 2/2N_e]_{\kappa \tan \kappa}}{[2N_o/2N_o - 2]_{\kappa \cot \kappa} + [2N_e + 2/2N_e]_{\kappa \tan \kappa}}. \quad (54)$$

Furthermore, for  $h\xi \ll 1$ , there holds

$$\omega_{hp}(\xi)^2 = \xi^2 + \left[ \frac{p!}{(2p)!} \right]^2 \frac{h^{2p}\xi^{2p+2}}{2p+1} + \dots \quad (55)$$



Order $p$	$R_p(h\omega_{hp})$	$\omega_{hp}(\xi)^2 - \xi^2$
1	$\frac{-2(h\omega_{h1})^2 + 6}{(h\omega_{h1})^2 + 6}$	$\frac{h^2\xi^4}{12}$
2	$\frac{3(h\omega_{h2})^4 - 104(h\omega_{h2})^2 + 240}{(h\omega_{h2})^4 + 16(h\omega_{h2})^2 + 240}$	$\frac{h^4\xi^6}{720}$
3	$\frac{-4(h\omega_{h3})^6 + 540(h\omega_{h3})^4 - 11520(h\omega_{h3})^2 + 25200}{(h\omega_{h3})^6 + 30(h\omega_{h3})^4 + 1080(h\omega_{h3})^2 + 25200}$	$\frac{h^6\xi^8}{100800}$
$p$		$\left[\frac{p!}{(2p)!}\right]^2 \frac{h^{2p}\xi^{2p+2}}{2p+1}$

Table 1: Special cases of relationship between  $\omega_{hp}(\xi)$  and  $\xi$  for order  $p$  approximation given in Theorem 1, along with the leading term for the error valid for  $h\xi \ll 1$ .

The relevant Padé approximants for the lowest order ( $p = 1$ ) elements coincide with Taylor polynomials and are given by

$$[2N_o/2N_o - 2]_{\kappa \cot \kappa} = 1 - \frac{1}{3}\kappa^2; \quad [2N_e + 2/2N_e]_{\kappa \tan \kappa} = \kappa^2$$

and, inserting these into equation (54) and simplifying, this leads to equation (52). Special cases of this result for orders  $p = 1, \dots, 4$  are given in Table 1, along with the leading term in the error valid for  $h\xi \ll 1$ . It is a simple matter to generate the corresponding result for higher orders of approximation using an algebraic manipulation package. An immediate consequence of the expression (55) for the error is that

$$\frac{\omega_{hp}(\xi)}{\xi} - 1 = \left[\frac{p!}{(2p)!}\right]^2 \frac{(h\xi)^{2p}}{2(2p+1)} + \dots \quad (56)$$

which, in the case  $p = 1$ , reduces to the result given by Thompson and Pinsky [24, eq. (41)]. Moreover, in the case of general order  $p$ , (55) has the form

$$\frac{\omega_{hp}(\xi)}{\xi} - 1 = \mathcal{O}(h\xi)^{2p} \quad (57)$$

conjectured by Thompson and Pinsky [24] on the basis of investigations of the particular cases  $p = 1, \dots, 5$ .

### 5.1 Order of accuracy of Nédélec elements for small wave number

It is now a simple matter to deduce the accuracy of the discrete dispersion relation for Nédélec element approximation of the time-harmonic Maxwell equations. Inserting the expressions for the discrete eigenvalues gives the discrete dispersion relation for  $p$ -th order Nédélec elements gives the following generalisation of equation (43). If  $h|\boldsymbol{\xi}_{hp}| \ll 1$ , then

$$\omega^2 = |\boldsymbol{\xi}_{hp}|^2 + \left[\frac{p!}{(2p)!}\right]^2 \frac{h^{2p}}{2p+1} [(\xi_1)^{2p+2} + (\xi_2)^{2p+2} + (\xi_3)^{2p+2}] + \dots \quad (58)$$

which demonstrates that  $p$ -th degree elements give a  $2p$ -th order accurate approximation of the dispersion relation for the time-harmonic Maxwell equations.

## 5.2 Behaviour for large wave number

The restriction on  $h|\xi_{hp}|$  is unrealistic in practical computations at higher wave number, where one would typically be obliged to work in the regime where  $\omega h \gg 1$ . The rapid decrease in the coefficient of the leading term in the error in the case  $\omega h \ll 1$  provides some hope that the scheme may be accurate for a larger range of wave number. Fig. 8 shows the behaviour of  $\cos(\omega h)$  and the rational function  $R_p(\omega_{hp}h)$  of equation (54) for order of approximation  $p = 1 \dots 10$  and  $\omega h \in [0, 20]$ . The figures confirm that the higher order methods continue to provide an accurate approximation even where  $\omega h$  is quite large, and moreover, as the order  $p$  is increased, the method appears to provide accurate resolution for an increasingly large range for  $\omega h$ .

Closer inspection leads to the conjecture that a  $p$ -th order method provides a reasonable approximation for values of  $\omega h$  up to approximately  $2p + 1$ . This question is studied in detail in [1], where the following result is shown: if  $\omega h \ll 2p + 1$ , then

$$\cos(h\omega_{hp}) - \cos(h\xi) \approx \frac{1}{2} \sin(\omega h) \left[ \frac{e\omega h}{2(2p+1)} \right]^{2p+1} + \dots \quad (59)$$

This estimate agrees with the upper bounds obtained by Babuška and Ihlenburg [17, Theorem 3.2]:

$$|\omega_{hp} - \omega| \leq \omega C C_a(p)^2 \left[ \frac{h\omega}{2p} \right]^{2p}, \quad \omega h < 1 \quad (60)$$

where  $C$  (respectively  $C_a(p)$ ) is a generic constant (respectively function of  $p$ ) defined in [17].

Estimate (59) provides a sharp quantification of the behaviour observed in Fig. 8, and reveals that as the order of the method is increased for a fixed value of  $\omega h$ , then one obtains a *super-exponential* decay in the error. Moreover, comparison with the results presented in Fig. 8 shows that the  $p$ -th order method provides an accurate approximation of the dispersion relation in the regime  $\omega h \in [0, 2p + 1]$ . Detailed analytical investigations given in [1] confirm the correctness of this observation for large order  $p$ . In addition, a detailed description is given of the precise nature of the transition between the super-exponential accuracy and the rapid degradation in accuracy observed in Fig. 8 when  $\omega h$  exceeds this threshold. The interested reader is referred to the above article for further details.

## 6 Conclusions

In conclusion, a simple argument has been presented showing that the discrete dispersion relation may be expressed in terms of the discrete dispersion relation for the approximation of the scalar Helmholtz equation in one dimension. An

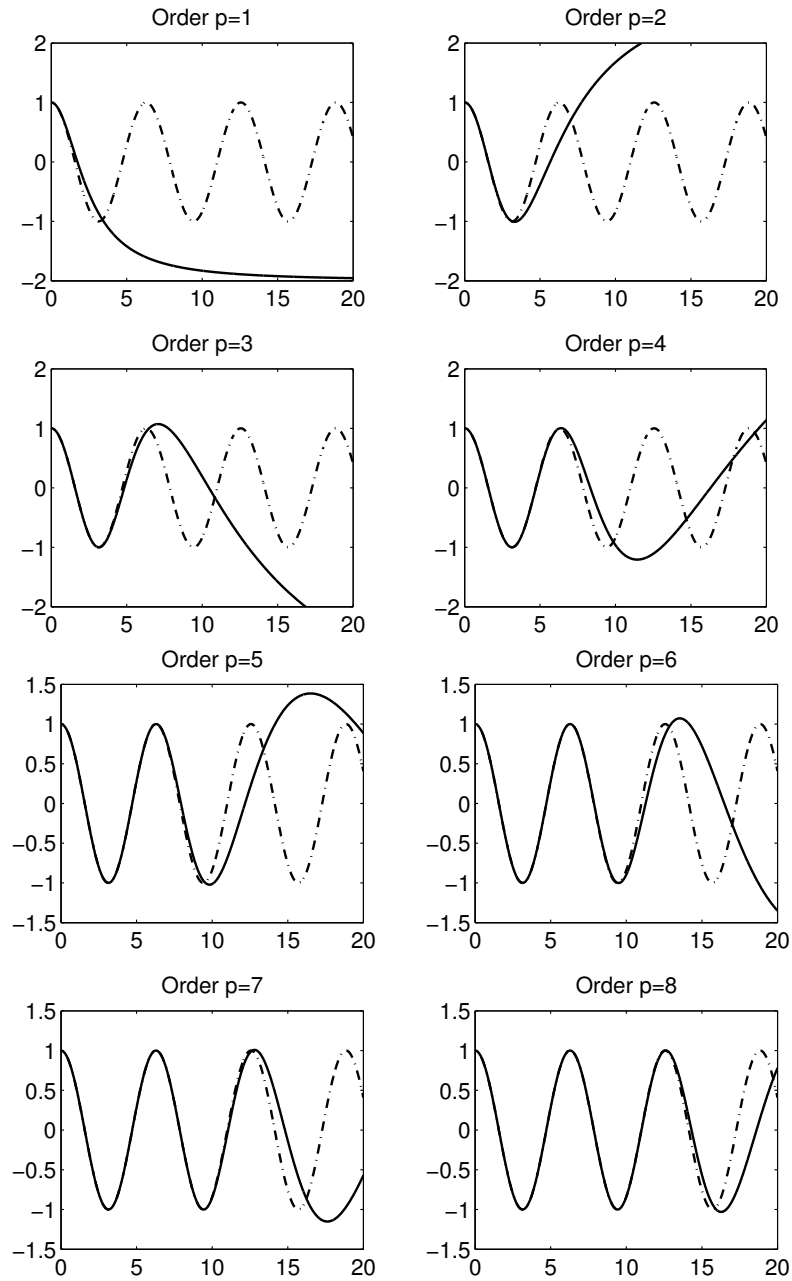


Figure 8: Curves for  $\cos(\omega h)$  (dashed line) compared with rational approximation  $R_p(\omega h)$  given in (54) (solid line), for methods of order  $p = 1$  to  $p = 8$ .

explicit form for the one dimensional dispersion relation was given, valid for arbitrary order of approximation. Explicit expressions for the leading term in the error in the regimes where (a)  $\omega h$  is small, showing that the dispersion relation is accurate to order  $2p$  for a  $p$ -th order method; and (b) in the high wave number limit where  $1 \ll \omega h \leq 2p + 1$ , showing that in this case the error reduces at a super-exponential rate as the order of approximation is increased.

These results shed light on the behaviour of higher order spectral element and  $p$ -version finite element methods for the approximation of the time-harmonic Maxwell equations at moderately high wave numbers, and provide quantitative information on the level of mesh refinement and order of approximation needed to control the dispersive effects. Moreover, the error estimates are sharp and provide lower bounds below which the dispersive behaviour will dominate. This establishes practical limits on the applicability of high order methods, beyond which the performance degenerates rapidly to the extent that the numerically computed wave is severely degraded by numerical dispersion.

**Acknowledgements** The author wishes to thank Dr Joe Coyle of Monmouth University for providing the data reported in the numerical example presented here. The support of this work by the Engineering and Physical Sciences Research Council of Great Britain under grant GR/M59426 is gratefully acknowledged.

## References

- [1] M. Ainsworth. Discrete dispersion relation for  $hp$ -version finite element approximation at high wave number. Technical Report 5, Strathclyde University, 2003.
- [2] M. Ainsworth and J. Coyle. Hierarchic  $hp$ -edge element families for Maxwell's equations on hybrid quadrilateral/triangular meshes. *Comput. Methods Appl. Mech. Engrg.*, 190:6709–6733, 2001.
- [3] M. Ainsworth and J. Coyle. Conditioning of hierarchic  $p$ -version Nedelec element on meshes of curvilinear quadrilaterals and hexahedra. *SIAM J. Numer. Anal.*, accepted for publication.
- [4] M. Ainsworth and W. Dörfler. Fundamental systems of numerical schemes for linear convection-diffusion equations and their relationship to accuracy. *Computing*, 66:199–229, 2001.
- [5] I. Babuška and F. Ihlenburg. Dispersion analysis and error estimation of Galerkin finite element methods for the Helmholtz equation. *Internat. J. Numer. Methods Engrg.*, 38:3745–3774, 1995.
- [6] I. Babuška and S.A. Sauter. Is the pollution effect of the FEM avoidable for the Helmholtz equation considering high wave numbers? *SIAM J. Numer. Anal.*, 34(6):2392–2423, December 1997.

- [7] M.A. Christon. The influence of the mass matrix on the dispersive nature of the semi-discrete, second-order wave equation. *Comput. Methods Appl. Mech. Engrg.*, 173:146–166, 1999.
- [8] P. G. Ciarlet. *The Finite Element Method for Elliptic Problems*. Elsevier, North-Holland, 1978.
- [9] G. Cohen and P. Monk. Gauss point mass lumping schemes for Maxwell’s equations. *Numer. Meth. PDE.*, 14:63–88, 1998.
- [10] G. Cohen and P. Monk. Mur-Nédélec finite element schemes for Maxwell’s equations. *Comput. Methods Appl. Mech. Engrg.*, 169:197–217, 1999.
- [11] G.C. Cohen. *Higher-Order Numerical Methods for Transient Wave Equations*. Springer Series in Scientific Computation. Springer-Verlag, Berlin, Heidelberg, New York, 2002.
- [12] M. Costabel and M. Dauge. Computation of resonance frequencies for maxwell equations in non-smooth domains. In M. Ainsworth, P.J. Davies, D.B. Duncan, P.A. Martin, and B.P. Rynne, editors, *Topics in Computational Wave Propagation: Direct and Inverse Problems*, Lecture Notes in Science and Engineering. Springer-Verlag, Heidelberg, 2003.
- [13] L. Demkowicz and L. Vardapetyan. Modeling of electromagnetic absorption/scattering problems using hp-adaptive finite elements. *Comput. Methods Appl. Mech. Engrg.*, 152(1-2):103–124, 1998.
- [14] J.S. Hesthaven and T. Warburton. Nodal high-order methods on unstructured grids. I. Time-domain solution of Maxwell’s equations. *J. Comput. Phys.*, 181(1):186–221, September 2002.
- [15] F. Ihlenburg. *Finite element analysis of acoustic scattering*, volume 132 of *Applied Mathematical Sciences*. Springer-Verlag, Berlin, 1998.
- [16] F. Ihlenburg. The medium frequency range in computational acoustics: practical and numerical aspects. *J. Comput. Acoust.*, accepted for publication.
- [17] F. Ihlenburg and I. Babuška. Finite element solution of the Helmholtz equation with high wave number. Part 2. The h-p version of the finite element method. *SIAM J. Numer. Anal.*, 34(1):315–358, 1997.
- [18] F. Ihlenburg, I. Babuška, and S. Sauter. Reliability of finite element methods for the numerical computation of waves. *Adv. Eng. Soft.*, 28(7):417–424, October 1997.
- [19] J. Jin. *The Finite Element Method in Electromagnetics*. John Wiley & Sons, Inc, 1993.
- [20] P.B. Monk and A.K. Parrott. Dispersion analysis of finite element methods for Maxwell’s equations. *SIAM J. Sci. Comput.*, 15(4):916–937, 1994.

- [21] J. Nédélec. Mixed finite elements in  $\mathbb{R}^3$ . *Numer. Math.*, 93:315–341, 1980.
- [22] F. Odeh and J.B. Keller. Partial differential equations with periodic coefficients and Bloch waves in crystals. *J. Math. Phys.*, 5(11):1499–1504, November 1964.
- [23] W. Rachowicz and L. Demkowicz. A two dimensional hp-adaptive finite element package for electromagnetics. *Comput. Methods Appl. Mech. Engrg.*, 93:315–341, 1999.
- [24] L.L. Thompson and P.M. Pinsky. Complex wavenumber Fourier analysis of the  $p$ -version finite element method. *Comput. Mech.*, 13:255–275, 1994.